

1 **Remapping Carbon Storage Change in Retired Farmlands on the Loess Plateau in**
2 **China from 2000 to 2021 in High Spatiotemporal Resolution**

3

4 Bingqian Guo¹, Mingjie Fang¹, Leilei Yang¹, Tao Guo¹, Chuang Ma¹, Xiangyun Hu¹, Zhaoxiang
5 Guo¹, Zemeng Ma¹, Qiang Li^{1,2*}, Zhaoli Wang³, Weiguo Liu^{1,2*}

6

7 ¹ Center for Ecological Forecasting and Global Change, College of Forestry, Northwest
8 Agriculture and Forestry University, Yangling, Shaanxi 712100, China.

9 ² Qinling National Forest Ecosystem Research Station, Yangling, Shaanxi 712100, China

10 ³ North West Inventory and Planning Institute of National Forestry and Grassland Administration

11 * Corresponding Author:

12 Qiang Li, Email: qiang.li@nwafu.edu.cn;

13 Weiguo Liu, Email: liuweiguo110@nwafu.edu.cn.

14

15

16 **Abstract:** The soil organic carbon pool is a crucial component of carbon storage in terrestrial
17 ecosystems, playing a key role in regulating the carbon cycle and mitigating atmospheric CO₂
18 concentration increases. To combat soil degradation and enhance soil organic carbon ~~sequestration~~ on
19 the Loess Plateau, the Grain-for-Green Program (GFGP) has been implemented. Accurately
20 quantifying ~~change in carbon capture and storage~~ soil organic carbon stock ~~–(CCSΔSOC)~~ resulting
21 from farmland retirement is essential for informing land use management. In this study, the spatial and
22 temporal distribution of retired farmlands on the Loess Plateau was analyzed using Landsat imagery
23 from 1999 to 2021. To assess the effects of the ~~length of farmland retirement~~ years since retirement,
24 climate, soil properties, elevation, and other factors on CCSΔSOC, climate-zone-specific multivariable
25 linear regression models were developed based on field-sampled soil data. These models were then
26 used to map ~~the dataset of CCSΔSOC~~ across the retired farmlands. Results indicated d that a total of
27 39,065 km² of farmland was retired over the past two decades, with 45.61% converted to grasslands,
28 29.75% to shrublands, and 24.64% to forestlands. The ~~length of farmland retirement~~ years since
29 retirement showed a significant positive correlation with CCSΔSOC, and distinct models were
30 developed for different climatic zones to achieve high-resolution (30 m) CCSΔSOC mapping. The total
31 CCSΔSOC from retired farmland on the Loess Plateau was estimated at 21.77 Tg in carbon equivalent–
32 ~~according to the dataset~~, with grasslands contributing 81.10%, followed by forestlands (11.16%) and
33 shrublands (7.74%).

34 **Keywords:** ~~Length of farmland retirement~~ Years since retirement; ~~carbon capture and storage~~ soil
35 organic carbon; ecological restoration; land use change; grain-for-green

36
37

38 1. Introduction

39 Soil organic carbon (SOC), as the largest terrestrial ecosystem carbon pool, plays a crucial role in
40 regulating climate change (Mir et al., 2023). Global SOC was estimated at approximately 1,400–1,500
41 Pg C, about four times the organic carbon pool of terrestrial plants (Scharlemann et al., 2014). The high
42 SOC is essential to support multiple ecological benefits, such as purifying water, increasing crop yields
43 and maintaining primary productivity (Paustian et al., 2019). Currently, 1/3 soil in the world is
44 degraded, causing many socioeconomic (e.g., unemployment, poverty, immigration) and environmental
45 (e.g., desertification, ecosystem degradation, biodiversity loss) issues (Ferreira et al., 2022; Ouyang et
46 al., 2016). The large area of degraded soil also released more than 50 Pg carbon ~~per year~~ annually into
47 the atmosphere which ~~is~~ conflicts with the decarbonization target for mitigating global warming
48 (Práválie et al., 2021). Therefore, ~~the restoration of~~ degraded soil is urgently needed for sustainable
49 development and environment ~~security~~ safety.

50 Ecological restoration by nature alone is a lengthy process. Under the urgent need for restoring
51 degraded soils and mitigating climate change, scientific management measures are necessary to
52 accelerate the ecosystem restoration process (Lengefeld et al., 2020; Pape, 2022; Wang et al., 2021a).
53 Many large-scale ecological restoration strategies around the world have showed encouraging
54 ecological benefits. Brazil's Atlantic Forest Restoration Pact (AFRP) was established in 2009, and
55 Argentina and Paraguay joined the impressive project in 2018, forming the Atlantic Forest Restoration
56 Tri-national Network (Calmon et al., 2011). Hundreds of organizations have been actively involved in
57 this decade-long efforts to protect and restore the forests, which recovered about 7,000 km² forests and
58 enhanced regional biodiversity (De Oliveira Faria and Magrini, 2016). Forests established by
59 restoration ~~of the Brazilian Atlantic Forest in this project~~ between 2010 and 2015 would have
60 sequestered 1.75 Pg carbon if they were not re-cut (Piffer et al., 2022). The Development Project
61 “Green Great Wall” in Africa was launched by the African Union in 2007, aiming at restoring
62 savannahs, grasslands and farmlands across Africa to help biodiversity cope with climate change and
63 desertification. The goals of the project are to restore 1,000,000 million km² forests in 2030 and
64 sequester 250 Tg C (Graham, 2022; Macia et al., 2023). China has started ecological restoration
65 practices and researches since the 1970s, and has implemented six national key ecological restoration
66 projects (Cui et al., 2021). Among the projects, the Grain-for-Green Program (GFGP) ~~GFGP~~ is one of
67 the most ambitious projects in the world with the highest investment and the largest implemented area
68 (Xu et al., 2022). From 1999 to 2019, the GFGP implemented in 25 provinces and exceeded 0.343
69 million km² land area with 49 Tg sequestered carbon, indicating a significant potential of ~~carbon-~~
70 ~~capture and storage~~ SOC stock ~~-(CCS)~~ by ecological restoration (Lu et al., 2018). Based on Deng et
71 al.'s (2017) study, the total carbon stock in the GFGP ~~affected~~ implemented area was 682 Tg C in

72 2010, and projected to 1,697 Tg C in 2020.

73 One of the primary area of the GFGP is the Loess Plateau, because the long-term indiscriminate
74 cultivation and logging on the Loess Plateau has caused over 40% of the total area (about 270,000 km²)
75 in severe soil erosion and a significant loss of ~~organic carbon~~SOC (Shao et al., 2022). As the
76 implementation of the GFGP, 96.1 Tg C was sequestered from 2000 to 2008 on the Loess Plateau
77 (Feng et al., 2013; Xiao, 2014). Nonetheless, current estimations of ~~CCS~~SOC stock still have large
78 uncertainties due to the technology and data limits (Zhang et al., 2022). On the Loess Plateau, the
79 accumulation of SOC can be affected by many untested factors, such as ecosystem types and ~~length of~~
80 ~~farmland retirement~~years since retirement. Moreover, most of the studies fail to differentiate the carbon
81 sequestration between retired and ~~in use~~currently cultivated farmlands, and caused an overestimate of ~~CCS~~
82 ~~SOC stock~~SOC stock. Therefore, a more reliable estimation should be reached to quantify the ~~CCS~~benefit in
83 SOC stock of the retired farmlands with the consideration of those issues (Deng et al., 2017; Sun et al.,
84 2016).

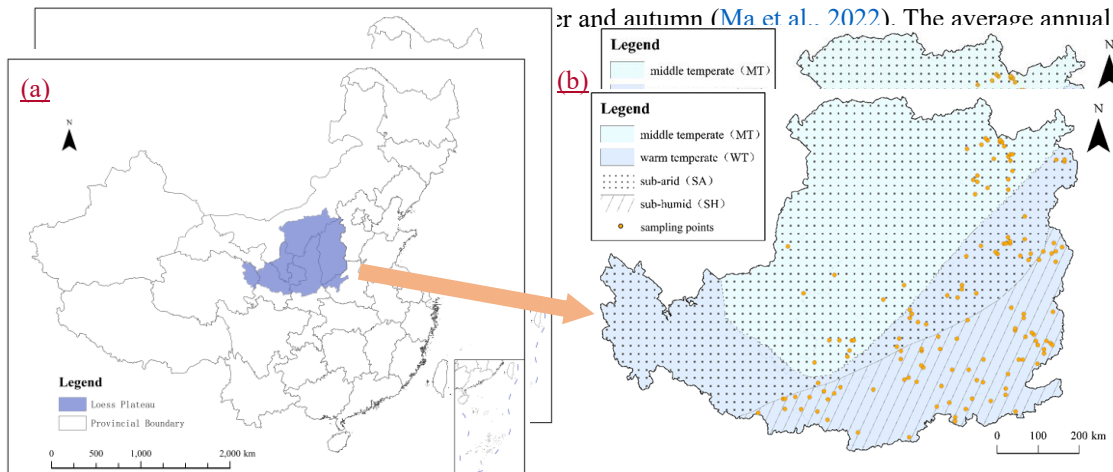
85 ~~Regarding to the complex spatial heterogeneity on the Loess Plateau and long time~~
86 ~~implementation of the GFGP (Ma et al., 2022), the change of SOC in high resolution since the~~
87 ~~implementation of the GFGP is essential to clarify the CCS from large scale ecological restoration, and~~
88 ~~can provide scientific guidance for ecological restoration policy and land use management on the Loess~~
89 ~~Plateau and sustainable utilization of vegetation resources. With the advancing of remote sensing~~
90 ~~technology and well designed sample scheme, the objectives of this study are: 1) to identify the year~~
91 ~~by year retirement of farmlands on the Loess Plateau from 2000 to 2021; 2) to develop models of CCS~~
92 ~~for the retired farmlands contributed by the GFGP; 3) to map the CCS in 30 m resolution and estimate~~
93 ~~the total CCS from the retired farmlands on the Loess Plateau after the implementation of the GFGP.~~
94 While previous studies have confirmed the overall increasing trend of SOC changes following
95 farmland retirement, significant uncertainties persist due to limited spatial resolution and insufficient
96 temporal coverage. Existing datasets fail to provide the continuous spatiotemporal dynamics of retired
97 farmland distribution on the Loess Plateau (Xu et al., 2018; Yang and Huang, 2021; Bai et al., 2024).
98 Furthermore, existing SOC assessments (Li et al., 2020; Yi et al., 2023) lack the capacity to quantify
99 fine-scale differences in SOC stock between retired and cultivated farmlands (Δ SOC). They also fail to
100 capture the year-by-year dynamics of retired farmlands and SOC accumulation in high resolution by
101 considering the heterogeneity of the Loess Plateau. To address these gaps, this study aims to: 1)
102 reconstruct annual farmland retirement patterns (2000-2021) using multi-source remote sensing data; 2)
103 develop a high-resolution Δ SOC model integrating terrain, climate and vegetation covariates based on
104 the difference in SOC stock between retired and adjacent cultivated farmlands; and 3) generate 30 m
105 resolution Δ SOC maps to quantify the impact of GFGP on carbon sequestration. Our spatially explicit

106 [approach provides unprecedented insights for optimizing ecological restoration strategies in](#)
107 [heterogeneous landscapes.](#)

108 2. Materials and Methods

109 2.1 Study Area

110 The Loess Plateau (100°52'–114°33' E, 33°41'–41°16' N) is located in the north central part of
111 China (Fig. 1-a), in the middle reaches of the Yellow River, with a sensitive and fragile ecological
112 environment, belonging to the warm temperate continental monsoon climate, characterized by dry and



114 temperature is 3.6–14.3°C. The average annual precipitation is 400–600 mm, of which is concentrated
115 between July and September, and decreases from east to west and south to north (Zhou et al., 2016).
116 The annual evaporation is 1,400–2,100 mm, with a trend of low in the south and east, high in the north
117 and west. The elevation is 800–3,000 m, and the original surface vegetation mostly is grassland,
118 shrubland, deciduous broadleaf forest, and mixed broadleaf-conifer forest (Zhou et al., 2016). The total
119 area of the Loess Plateau is 635,000 km², including Shanxi, Ningxia, Shaanxi, Gansu, Qinghai, Inner
120 Mongolia, Henan provinces. The main terrain is hilly and gully, with soft loessial soil texture.

121
122 **Figure 1. The map of the study area, (a) location, (b) soil sampling sites and (c) climate-**
123 **zone climatic zones.**

124 2.2 Identifying Retired Farmlands

125 To identify and confirm the spatial range of the annual retired farmlands on the Loess Plateau,
126 Landsat remote sensing images (30 m resolution) from 1999 to 2021 were downloaded from the United
127 States Geological Survey (USGS, <https://EarthExplorer.usgs.gov>). The images with less cloud (lower
128 than 10%) in growing season (from May to September) were selected for further analysis. Those
129 images were processed by the standard steps recommended by ArcGIS Pro 2.8 (Environmental
130 Systems Research Institute, Inc., ESRI), including preprocessing, image classification and validation.
131 To improve image readability, remote sensing images were first preprocessed in ENVI 5.3, including

132 radiometric calibration, FLAASH (Fast Line-of-sight Atmospheric Analysis of Spectral Hypercubes)
133 atmospheric correction, gram-schmidt pan sharpening, seamless mosaic and subset data from ROIs
134 (regions of interest). The image classification was then performed in ArcGIS Pro 2.8. In this study, we
135 used the support vector machine (SVM) supervised classification method to classify the land cover
136 types into the following seven categories: farmland, forestland, grassland, shrubland, water body,
137 building land, and bare land. Training samples were selected through visual interpretation of high-
138 resolution imageries and systematically managed using a training sample manager. A total of 23,100
139 ROI samples were used for model training, with an additional 6,930 independent ROIs reserved for
140 validation. During the accuracy assessment phase, the classification performance over the study period
141 consistently achieved kappa coefficients ranging from 0.76 to 0.90 and overall accuracy values
142 between 0.80 and 0.91. The average accuracies for different land cover types were as follows: farmland
143 (0.71), forestland (0.87), grassland (0.86), shrubland (0.92), water body (0.97), building land (0.92),
144 and bare land (0.87).The training samples were selected by visual interpretation and managed by
145 training sample manager. The training set comprised 23,100 ROI samples, and the validation set
146 contained 6,930 ROI samples. In the accuracy validation stage, the kappa coefficients for the studied
147 period were in a range of 0.76–0.90 and the overall accuracy were 0.80–0.91 for different land
148 cover types, per-class average accuracies were farmland (0.71), forestland (0.87), grassland (0.86),
149 shrubland (0.92), water body (0.97), building land (0.92), and bare land (0.87).

150 2.3 Field Sampling and SOC Measurements

151 To determine the Δ SOC in ecosystems established on retired farmlands, we implemented a
152 systematic sampling design based on spatial proximity principles. Initial sample sites were
153 systematically generated at 5-km intervals across the retired farmland distribution map (Fig. 1-b),
154 forming a comprehensive grid framework. For each retired farmland point, we identified the nearest
155 long-term cultivated farmland counterpart to create a spatially paired sampling site. The sampling
156 strategy incorporated stratification across different ecosystems, climatic zones, and years since
157 retirement. To minimize human interference, we pre-screened all potential sites using ultra-high
158 resolution imagery (0.5 m) to exclude areas near roads, villages, or irrigation ditches. Additional
159 considerations included accessibility and sampling feasibility, leading to the exclusion of 133 site pairs
160 from initial design to field implementation.To determine the CCS of different ecosystems that
161 established on retired farmlands, an initial set of sample sites were created evenly with 5 km gaps
162 based on the spatial distribution maps of retired farmlands (Fig. 1-b), design paired sample sites based
163 on the principle of spatial proximity. Considering covering different ecosystems, different climatic
164 zones, years since retirement, human interference (such as roads, villages, or ditches in disturbance
165 prone areas), accessibility, and the difficulty of sampling, and the final sample sites were determined by

166 ~~removing unqualified sites with ultra-high spatial resolution images (0.5 m resolution).~~ Finally, 2,430
167 soil samples from 135 sample sites were collected from fields. Nine soil samples (three 10-cm layers
168 from top 30 cm soil in 3 sample points) were collected for every sample site, and nine soil samples
169 from the nearest farmlands were also collected similarly. Each soil sample was individually bagged,
170 labeled, and stored in cold storage for lab measurement. After drying and grinding through a sieve at
171 0.25 mm, SOC of each soil sample was measured by potassium dichromate external heating method.
172 The difference in total SOC stock of the top 30 cm soil layer between retired farmlands and the nearest
173 cultivated farmlands was defined as CCSΔSOC that contributed by the GFGP.

174 2.4 Model Development and CCSΔSOC Mapping on the Loess Plateau

175 CCSΔSOC is influenced by both natural environmental conditions and human activities, leading
176 to variations across different climatic zones conditions of the Loess Plateau. Therefore, we developed
177 different models based on the relationships between CCSΔSOC and variables such as ~~length of-~~
178 ~~farmland retirement~~ years since retirement, geographic location, elevation, soil bulk density (BD),
179 ~~temperature, precipitation,~~ and 19 bioclimatic factors. Length of farmland retirement Years since
180 retirement were obtained from the annual spatial distribution data in retired farmlands on the Loess
181 Plateau (subsection 2.2). The data sources for climate information can be found in subsection 2.5. The
182 19 bioclimatic factors were derived by following the formula in WorldClim
183 (<https://worldclim.org/data/index.html>). For every grid cell of retired farmlands, the bioclimatic factors
184 were calculated as the average of the years since retirement. All the variables were extracted to the
185 sample sites by the Kriging interpolation and prepared for model development.

186 Based on the factors introduced above, we combined ~~correlation analysis, ANOVA, random forest,~~
187 ~~(The integration of randomness in data (Bagging) and randomness in features enables ensemble~~
188 ~~learning to construct multiple “decision trees” that collectively form a forest for decision making.) and~~
189 single-factor regression, all subset regression and stepwise regression to select variables for
190 multivariate linear models of CCSΔSOC. The steps included: data preprocessing, univariate analysis,
191 multivariate analysis, model evaluation, and diagnostic checks. Finally, several key variables that co-
192 occurred were selected. In consideration of wide climatic range on the Loess Plateau and different
193 possible response of CCSΔSOC to the ~~retirement~~ factors among climatic conditions (Zhang et al.,
194 2018), we divided the Loess Plateau into different climatic zones for different ecosystem types (e.g.,
195 forestland, shrubland, grassland) based on climate regionalization in China—Climatic zones and
196 climatic regions (GB/T 17297-1998) and climate data (subsection 2.5). As Fig. 1-c shows, we obtained
197 middle temperature zone (MT, < 8°C) and warm temperate zone (WT, > 8°C) by the annual average
198 temperature, and semi-arid zone (SA, <400 mm) and sub-humid zone (SH, >400 mm) by annual
199 precipitation. In addition, ~~five~~ three combined climatic zones were obtained: MT-SA (same as MT),

200 WT-SA ~~and~~, WT-SH (same as SH), WT, and SA. A multivariate linear regression model was developed
201 specifically for each ecosystem types in each climatic zone. Before regression analysis, diagnosis of
202 multicollinearity is conducted, and the threshold is generally set at 10 to detecting correlations between
203 the independent variables and identify those independent variables that were incorrectly included in the
204 same regression model. The regression models were evaluated and validated by residual analysis, ~~–~~
205 ~~cross validation~~, significance level (p -value), coefficient of determination (R^2), root mean square error
206 (RMSE) and mean absolute error (MAE), and the robustness of the models were validated by leave one
207 out-cross-validation. Statistical power analysis indicates that the current stratified sampling design
208 provides adequate power for detecting medium to large effects, though sensitivity for detecting small
209 effects remains limited. Model robustness under this design is rated as “acceptable”.

210 Based on the results of model evaluation, the ~~best fitted models were selected~~ final selected models
211 were used to estimate the overall CCSASOC of retired farmlands on the Loess Plateau. With the final
212 selected multivariate linear regression models, the CCSASOC in the top 30 cm soil layer were mapped
213 by raster calculation in different climatic zones and ecosystem types at 30 m resolution. And the total
214 CCSASOC on the Loess Plateau contributed by the GFGP was obtained by summing up the CCSASOC
215 in all the retired farmlands without ~~reclamation-recultivation~~ within the study period.

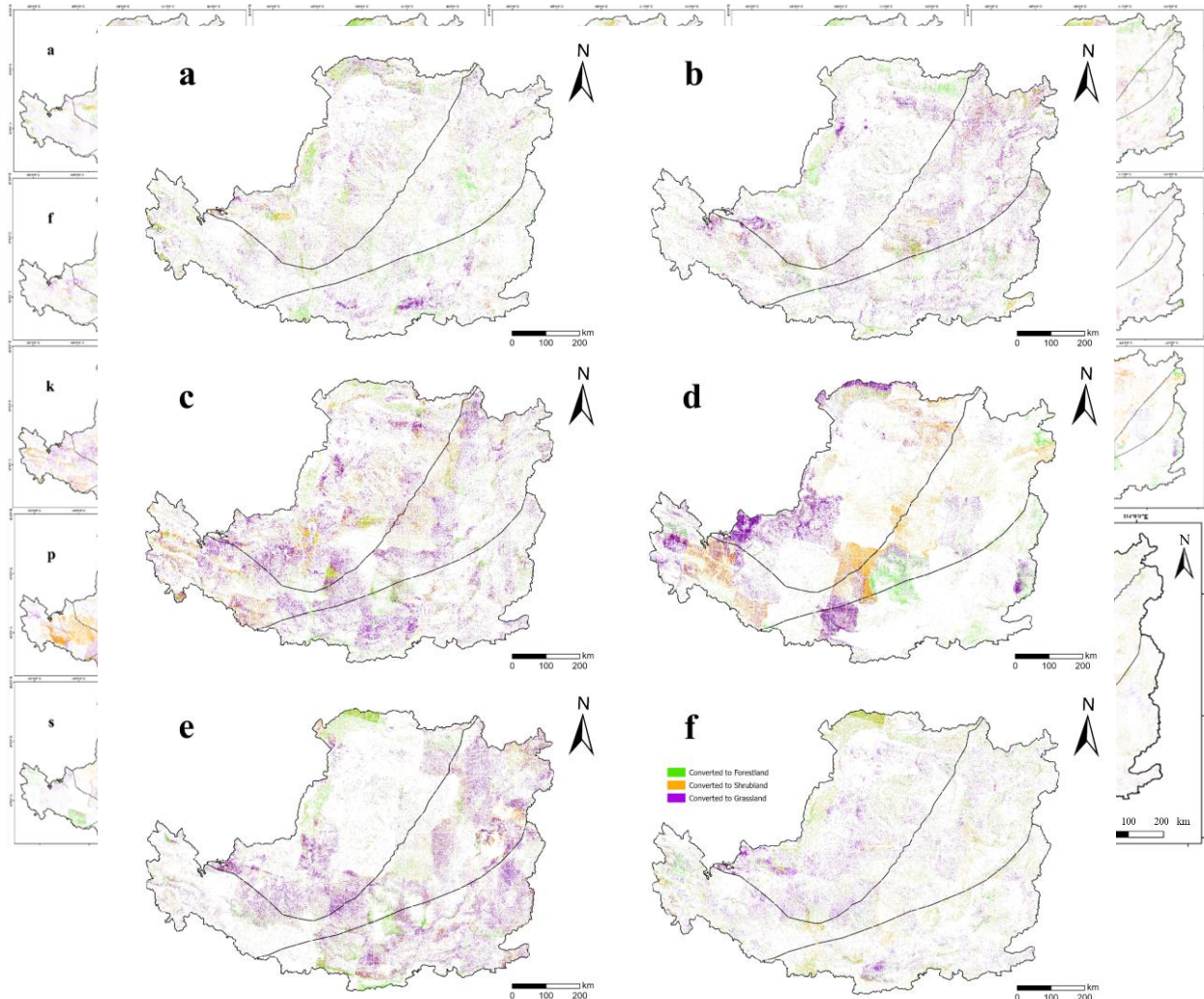
216 2.5 Data Sources

217 The air temperature and precipitation data to calculate the 19 bioclimatic factors were from the
218 China Meteorological Data Service Center (CMDSC, <http://www.geodata.cn>). Elevation data of every
219 grid cell were from the Digital Elevation Model database (<https://e4ftl01.cr.usgs.gov/MEASURES/>).
220 Soil properties were retrieved from Harmonized World Soil Database (HWSD,
221 [https://www.fao.org/soils-portal/soil-survey/soil-maps-and-databases/harmonized-world-soil-database-](https://www.fao.org/soils-portal/soil-survey/soil-maps-and-databases/harmonized-world-soil-database-v12/en/)
222 [v12/en/](https://www.fao.org/soils-portal/soil-survey/soil-maps-and-databases/harmonized-world-soil-database-v12/en/)), and the boundary of the Loess Plateau was downloaded from the Resource and Environment
223 Science and Data Center (<https://www.resdc.cn/>). All the raster data were resampled to 30 m resolution.

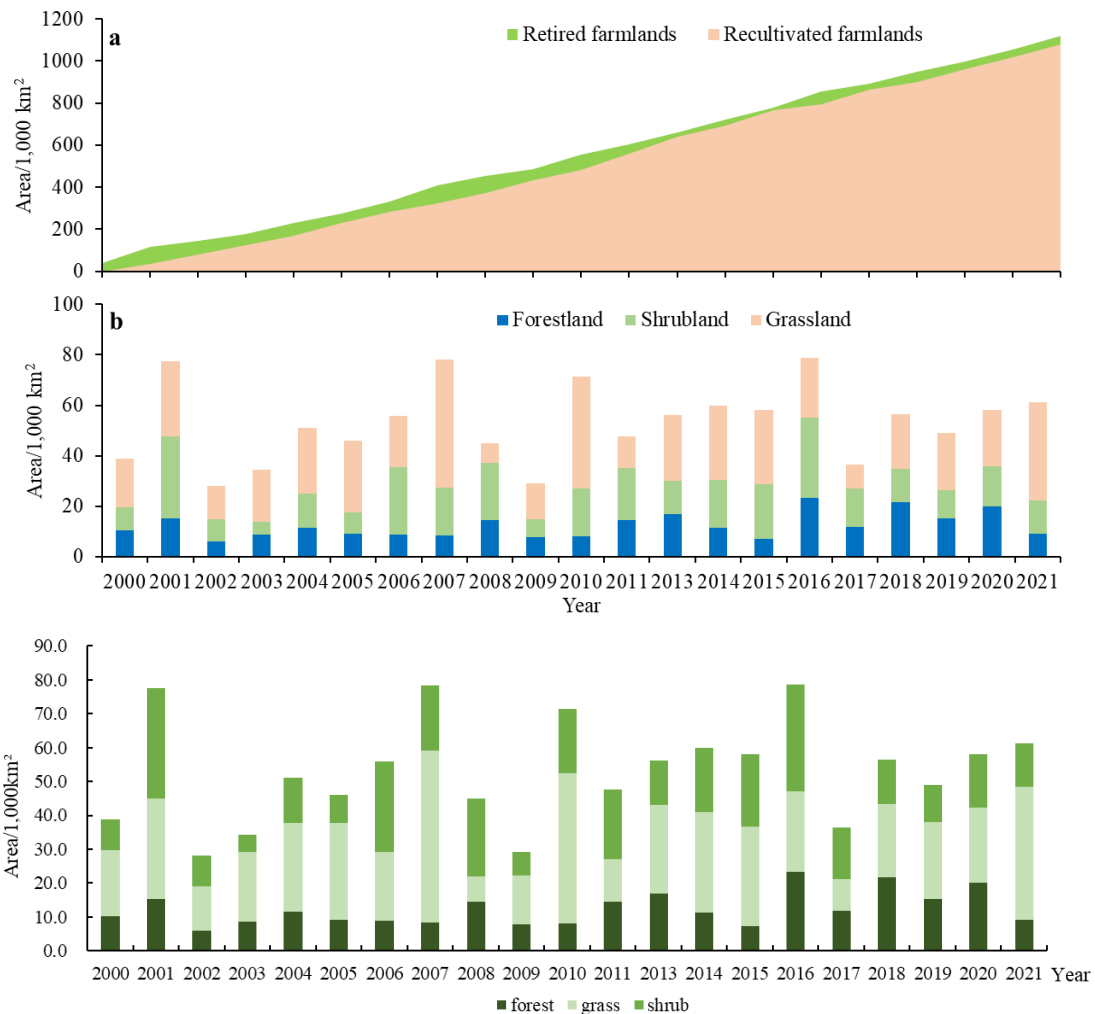
224 3. Results

225 3.1 Distribution of Retired Farmlands

226 From 1999 to 2021, the final retired farmlands without reclamation-recultivation on the Loess
 227 Plateau was 39,065 km² (Fig. 2-2-va). The final retired farmlands were less than the area by summing
 228 up yearly-annually retired farmlands because of frequent reclamation-recultivation (Fig. 3-a). The
 229 annual area of retired farmlands in every year has been fluctuating throughout the study period with no
 230 significant trend (Fig 2-2-a-u, Fig. 3-b). The least amount of retired farmlands occurred in 2002 (28,003
 231 km²; 4.41% of the whole studied area), and the most was 78,653 km² in 2016 (12.39% of the whole
 232 studied area). The retired farmlands were converted to different ecosystem-vegetation types, including
 233 forestlands, shrublands and grasslands. The ratios of different ecosystem-vegetation types in every year
 234 were in the ranges of 10.65%–38.60%, 14.63%–47.70% and 17.02%–64.98% for forestlands,
 235 shrublands and grasslands, respectively (Fig. 3-b). Within the studied period in average, most of the
 236 retired farmlands were converted to grasslands (45.61 %) and shrublands (29.75 %).



237
 238 **Figure 2. Spatial distribution of annually retired farmlands on the Loess Plateau ~~from 1999 to~~**
 239 **2021, in (a) 1999–2000, (b) 2000–2001, (c) 2001–2002, (d) 2002–2003, (e) 2003–2004, (f) 2004–2005,**
 240 **(g) 2005–2006, (h) 2006–2007, (i) 2007–2008, (j) 2008–2009, (k) 2009–2010, (l) 2010–2011, (m) 2011–**
 241 **2013, (n) 2013–2014, (o) 2014–2015, (p) 2015–2016, (q) 2016–2017, (r) 2017–2018, (s) 2018–2019,**



243

244 **Figure 3. a) Cumulative retired farmlands and recultivated farmlands and b) Annual area of**
 245 **different ecosystem-vegetation types from retired farmlands from 2000 to 2021.**

246 The annual retired farmlands were unevenly distributed among different climate zone climatic
 247 zones (Fig. 2-2-a-vf). The annual retired farmlands in the other years can be found in the supplementary
 248 material (Fig. S1 a-p). For the final retired farmlands, the area in the middle temperate and semi-arid
 249 zone (MT-SA), warm temperature and semi-arid zone (WT-SA) and warm temperature and semi-
 250 humid zone (WT-SH) were 20,299 km², 10,572 km² and 8,194 km², respectively. In the MT-SA zone,
 251 the dominant ecosystem type from retired farmlands was grasslands which had 9,705 km² (47.81%),
 252 and followed by shrublands (5,887 km², 29.00%) and forestlands (4,707 km², 23.19%). In the WT-SA
 253 zone, grasslands were also the dominant ecosystem type which accounted for 4,925 km² (46.59%), and
 254 forestlands accounted the least (2,384 km², 22.55%). In the WT-SH zone, the percentages of different
 255 ecosystem types were 30.96 %, 30.16 % and 38.88 % for forestlands, shrublands and grasslands,
 256 respectively.

257

Among different years (Fig. 2-2-a-u, Fig. S1), the highest areas for each ecosystem type were

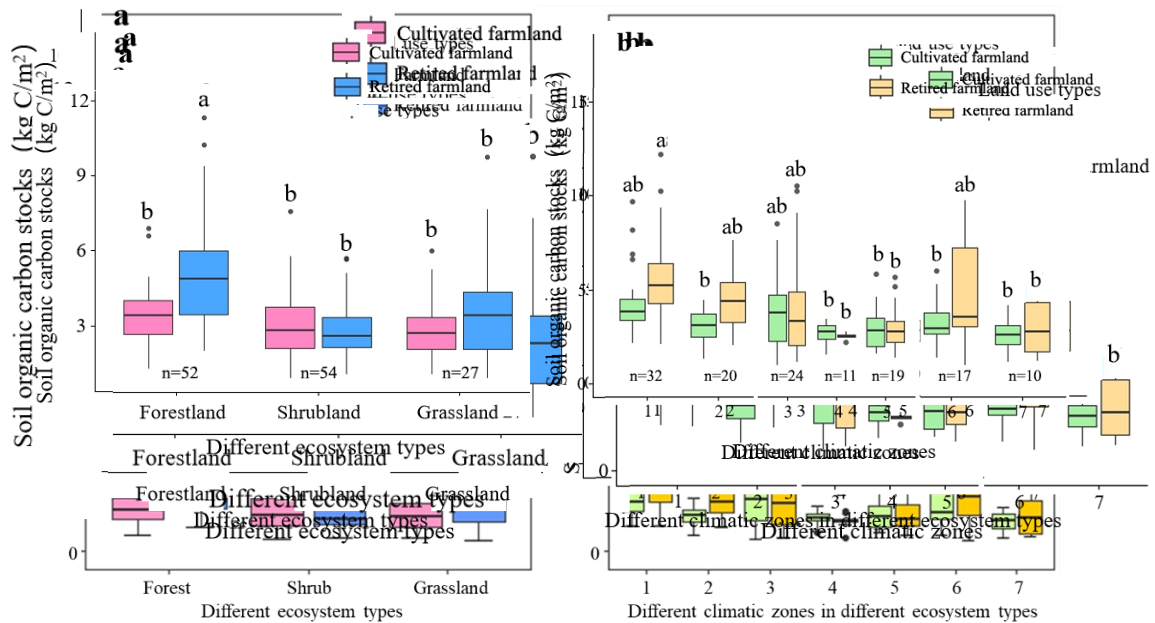
258 forestlands in the WT-SH zone in 2016 (12,846 km²), shrublands in the MT-SA zone in 2001 (15,441
259 km²), and grasslands in the MT-SA zone in 2007 (26,171 km²). The lowest areas were found in 2019
260 for forestlands in the WT-SA zone (813 km²), in 2013 for shrublands in the WT-SH zone (271 km²),
261 and in 2013 for grasslands in the WT-SH zone (806 km²).

262 Among provinces, the retired farmlands in different years had significant differences (Table S1),
263 where Shanxi Province had the most in 2016 (30,912 km²) and Qinghai Province had the least in 2017
264 (438 km²). The final retired farmlands from 1999-2021 was the most in Inner Mongolia Province
265 (8,626 km²) and the least in Henan Province (739 km²). More forestlands could be found in warmer
266 and wetter regions. The largest forestlands (15,073 km²) were found in Shanxi Province in 2016, while
267 the least were found in Qinghai Province in 2016 (34 km²).

268 3.2 Analysis of Soil Samples

269 The results of soil samples showed that the SOC stock were 2.19–62.70 g C/kg in retired
270 farmlands, and 2.25–63.83 g C/kg in adjacent cultivated farmlands. The average SOC were the highest
271 in forestlands (4.84–62.70 g C/kg), followed by shrublands (2.62–54.72 g C/kg) and grasslands (2.19–
272 21.83 g C/kg). The average Δ SOC of the all sample points was 2.86 g C kg⁻¹, with a standard error of
273 1.17 g C kg⁻¹, and a 95% confidence interval of [0.56, 5.15] g C kg⁻¹. The findings indicated that the
274 farmland retirement had significantly increased the SOC stock. To facilitate the $\text{CCS}\Delta\text{SOC}$ estimation
275 by area, we converted the SOC stock to area based content by soil bulk density. The highest value of
276 $\text{CCS}\Delta\text{SOC}$ after retirement was from forestlands in the SH zone (26.52 kg C/m²) and the lowest value
277 was from sample in grasslands in the WT zone (0.91 kg C/m²). Forestlands and shrublands had
278 significantly increased the SOC stock by 48.53% and 20.34%, respectively ($p < 0.05$, Fig. 4-4-a). Among
279 different climatic zones (Fig. 4-4-b), forestlands in the SA zone had the biggest increase (58.80%), and
280 followed by forestlands in the SH zone (44.53%) and shrublands in the MT-SA zone (26.74%). The
281 mean Δ SOC was 2.86 g C kg⁻¹, with a standard error of 1.17 g C kg⁻¹, and a 95% confidence interval of
282 [0.56, 5.15] g C kg⁻¹. The findings indicated that the farmland retirement had significantly increased
283 the SOC storage.

284 0The CCSΔSOC of different ecosystem types in different climatic zones had significant
 285 relationship to the length-of-farmland-retirement-years since retirement (Fig. 5). The CCSΔSOC was
 286 negative in the first few years and significantly increased as the length-of-farmland-retirement-years
 287 since retirement increases, except forestlands in the SA zone and shrublands in the MT-SA zone. Most
 288 of the relationships indicated constant increase in CCSΔSOC except CCSΔSOC in grasslands in the



289 MT zone which had a saturation point after 15 years of retirement.

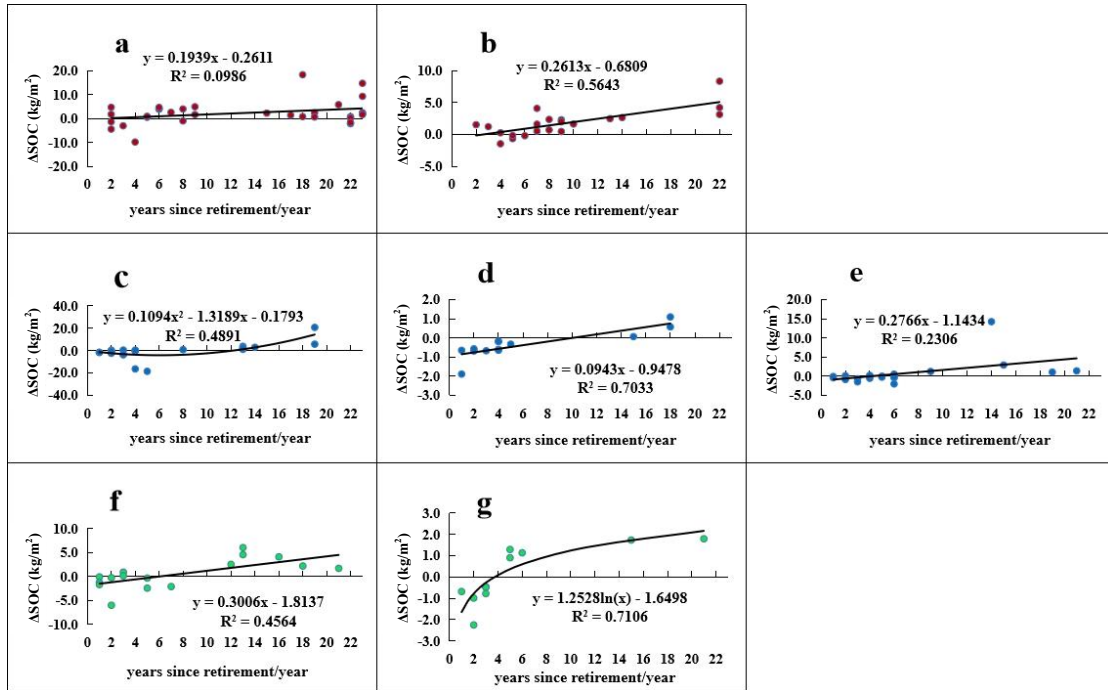
290

291 **Figure 4. SOC stocks in farmlands and retired farmlands ($g\text{-}C/kgC/m^2kg$), (a) Comparison**
 292 **of SOC stocks on the Loess Plateau in farmlands retired to different ecosystem types (forestland,**
 293 **shrubland, grassland) with those in adjacent cultivated farmlands, and letters a and b are labeled**
 294 **to indicate significant differences in the ANOVA. (b) Comparison of different climatic zones are**
 295 **emphasized.**

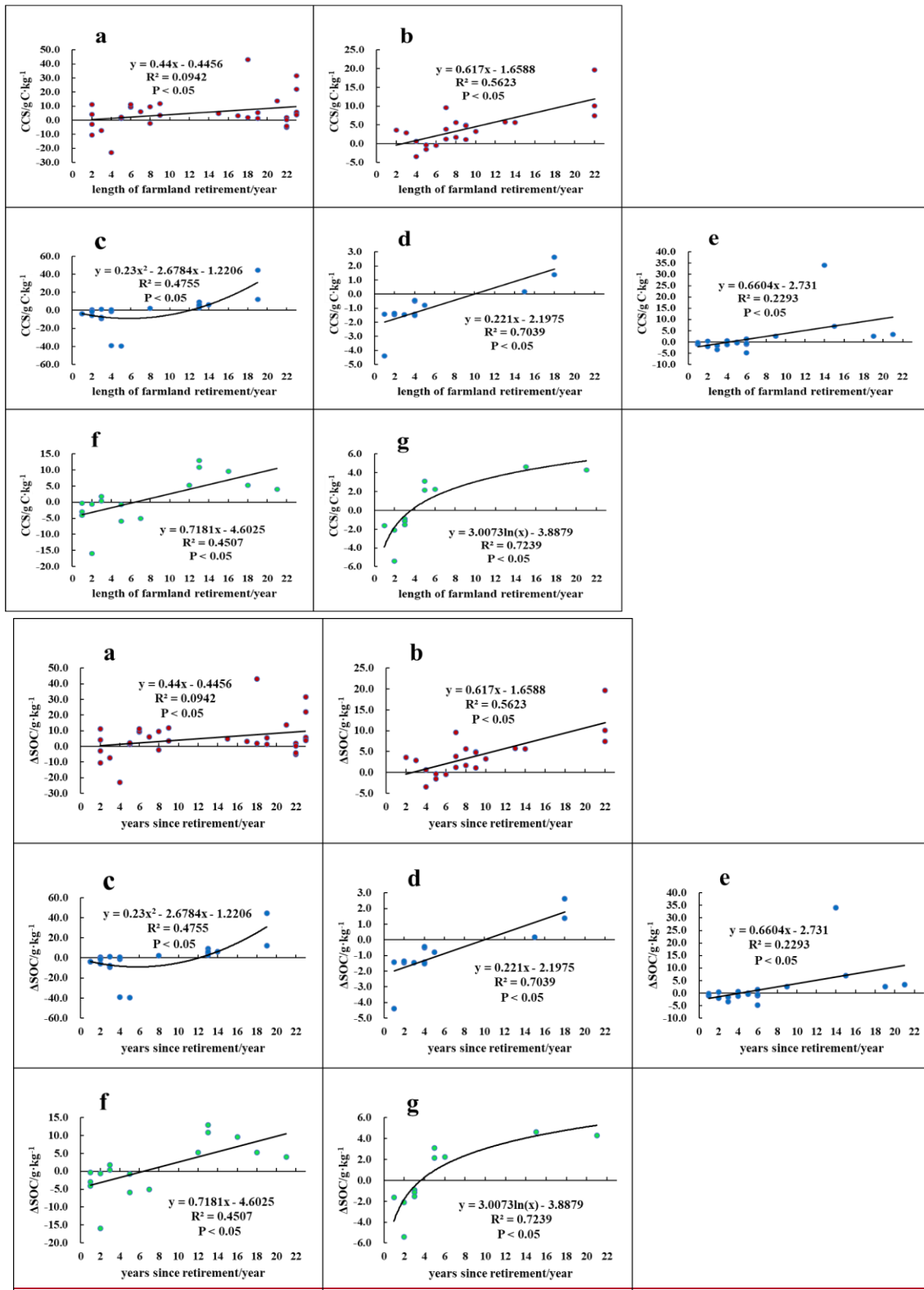
296 **Note: and 1-7 represent the climatic zones of the different ecosystem types, i.e., forestlands in**
 297 **the SH zone, 2-forestlands in the SA zone, 3-shrublands in the WT-SH zone, 4-shrublands in the**
 298 **WT-SA zone, 5-shrublands in MT-SA the zone, 6-grasslands in the WT zone, and 7-grasslands in**
 299 **the MT zone;**

300 **and letters a, and b and ab are labeled to indicate significant differences in the ANOVA, for**
 301 **same ecosystem in figure 1-a and for same climatic zone combination figure 1-b.**

302



303

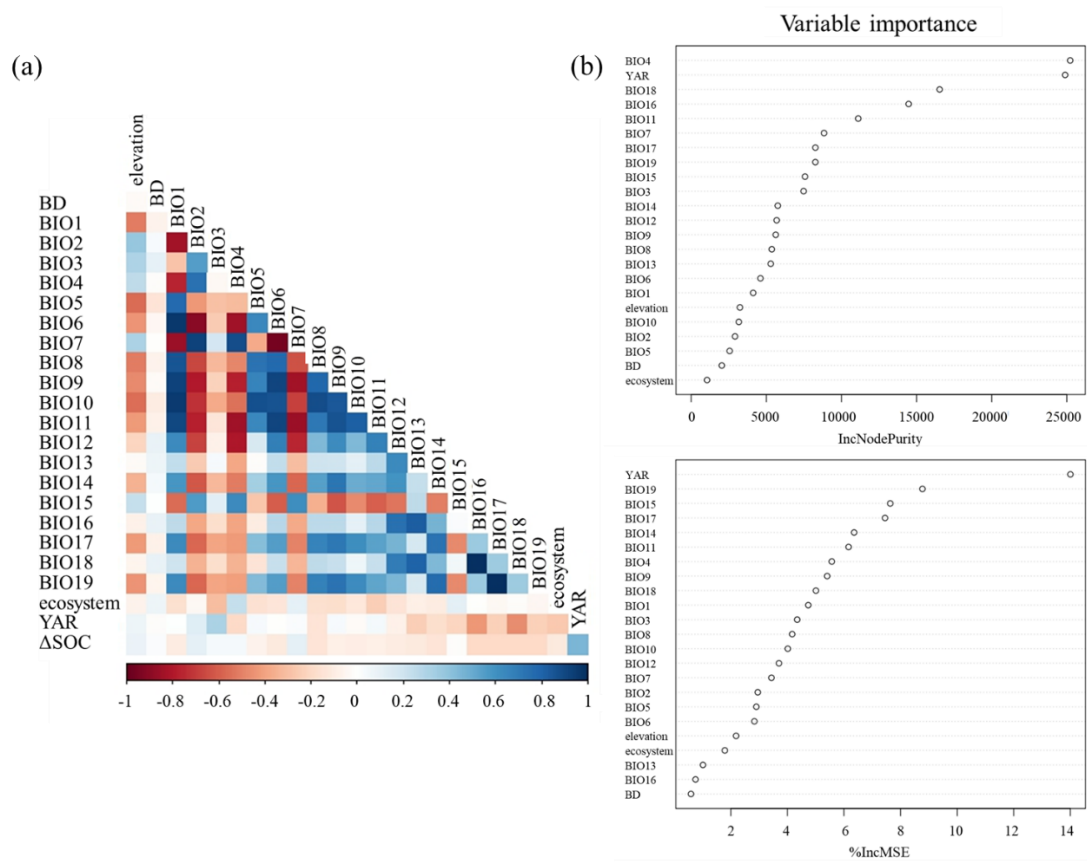


304
 305 **Figure 5. Relationship between length of farmland retirement years since retirement and**
 306 **CCSΔSOC**, (a) forestlands in the SH zone, (b) forestlands in the SA zone, (c) shrublands in
 307 **the WT-SH zone, (d) shrublands in the WT-SH zone, (e) shrublands in the MT-SH zone, (f)**
 308 **grasslands in the WT zone, (g) grasslands in the MT zone.**

309 3.3 Models of CCSΔSOC

310 3.3.1 Correlation analysis and variable importance

311 The critical variables for model development were selected by the Pearson correlation analysis
312 and variable importance through package *randomForest* in R. The length of farmland retirement and
313 CCS (Fig. 6 a) showed a significant positive correlation. Most of the environmental factors such as soil
314 bulk density and bioclimatic factors had a weak negative correlation with CCS. Variable importance
315 (Fig. 6 b) was measured in %IncMSE (percent increase in mean squared error) and IncNodePurity
316 (increase in node purity). The combination of the two metrics illustrated that the length of farmland
317 retirement on the Loess Plateau is the most important variable for CCS.
318



319

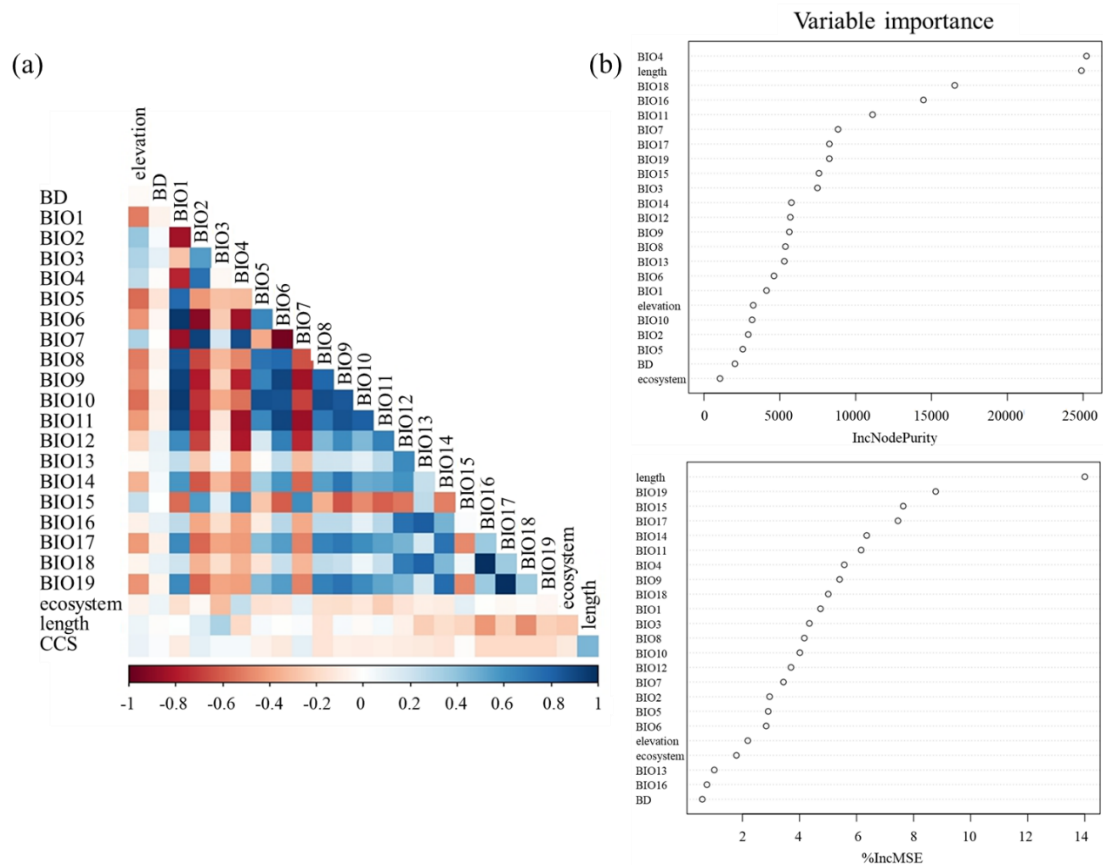


Figure 6. Correlation matrix (a) and variable importance (b) of CCS and environmental factor parameters. Where, BD is soil bulk density, and BIO1-BIO19 are 19 bioclimatic factors

3.3.2 Model development

Based on the results from correlation analysis and variable importance, all the factors significant contributing to the variance of CCS were introduced into the regression model. Samples for different ecosystem types were divided by different combinations of climatic zones to find the final selected optimal models by Backward Stepwise Regression. All variance inflation factor (VIF) diagnostic results were below the threshold of 10, including years since retirement, latitude, longitude, elevation, soil bulk density, and bioclimatic variables BIO1 to BIO19. The final selected models of CCSASOC in different ecosystem types were shown in Table 1 and Fig. S2 based on the results of evaluation and validation. In this table, *t* is the length of farmland retirement years since retirement, *lat* is latitude, *ele* is elevation, *BD* is soil bulk density, and *BIO1-BIO19* are 19 bioclimatic factors, *n* is sample sizes at each level.

The analysis showed that seven regression equations were the best-final acceptable representative for the CCSASOC on the Loess Plateau when the study area was divided into SH and SA zones for forestlands, WT-SH, WT-SA and MT-SA zones for shrublands, and WT and MT zones for grasslands. The coefficients of determination (R^2) ranged from 0.476 to 0.830 with $p < 0.05$. all variance inflation factor (VIF) diagnostic results were below the threshold of 10. The models with the highest R^2 were

339 obtained for grasslands (0.830 in the WT zone and 0.790 in the MT zone), and the model with the
 340 lowest R² was for shrublands in the MT zone (0.476).

341
 342
 343
 344
 345
 346
 347

Table 1 Models of the CCSASOC in retired farmlands on the Loess Plateau.

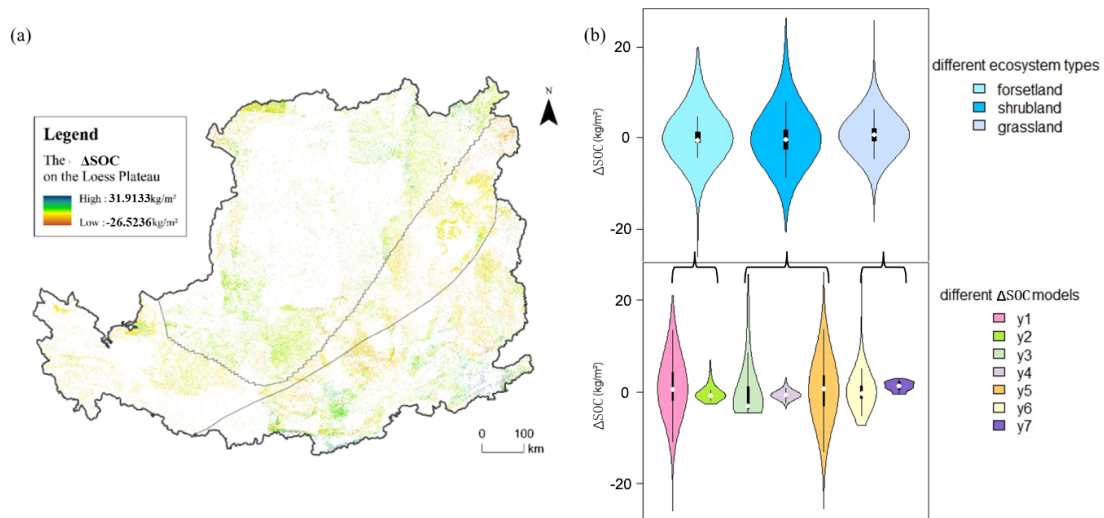
Ecosystem	Zone	Model	<u>n</u>	R ²	p-value	RMSE	MAE	
Forestland	SH	$y_1=0.3195 t+14.95 lat+0.01356 ele - 0.00755 BIO4 - 4.02 BIO5+11 BIO10+0.44 BIO13+1.791 BIO14 - 23.81 BIO15 - 1.686 BIO17-632$	<u>32</u>	0.605	<0.05	21.831	17.209	
	SA	$y_2=0.7384 t - 0.4148 BIO12+4.2594 BIO14 - 0.8341 BIO17+0.1456 BIO18+1.1633$	<u>240</u>	0.618	<0.01	9.039	7.001	
Shrubland	WT	SH	$y_3=0.23 t^2 - 2.678 t - 1.221$	<u>224</u>	0.476	<0.01	34.814	22.858
		SA	$y_4=0.1555 t - 1.4904 BIO1 - 0.1544 BIO17+15.3573$	<u>131</u>	0.773	<0.01	2.281	1.715
	MT	SA	$y_5=1.6059 t - 12.1498 BIO3+0.0071 BIO4+0.7615 BIO13 - 1.2096 BIO16+523.89$	<u>201</u> <u>9</u>	0.551	<0.05	48.965	36.664
Grassland	WT	$y_6=0.5457 t+31.412 BD+4.463 BIO9 - 2.489 BIO11 - 2.238 BIO14+27.184 BIO15 - 72.97$	<u>167</u>	0.830	<0.01	8.659	7.112	
	MT	$y_7=-0.0497 t^2+1.455 t - 4.84$	<u>140</u>	0.790	<0.01	4.114	2.898	

348 3.4 Mapping CCSASOC

349 According to the regression models for CCSASOC and the distribution of retired farmlands, the
 350 CCSASOC in the retired farmlands on the Loess Plateau was quantified throughout the GFGP

351 implementation period, excluding recultivated farmlands calculated (Fig. 7-6-a). The total benefit in CCSΔSOC
 352 on the Loess Plateau till 2021 was 21.77 Tg C with a range between -26.52 and 31.91 kg
 353 C/m² at 30 m raster level. Significant variations in ΔSOC were observed across different ecosystem
 354 types (Fig. 6-b, Table 2). To provide detailed and vegetation-specific insights, Table 2 presents ΔSOC
 355 values for three climatic zone combinations associated with each vegetation type. The potential CCS by
 356 different ecosystem types changed significantly (Fig. 7 b, Table 2). Grasslands contributed the most
 357 CCSΔSOC increment (17.657 Tg C). Among the different climatic zones for grasslands, MT zone
 358 contributed the most (78.04%, -0.48–3.04 kg C/m²), followed by WT zone (21.96%, -8.20–31.91 kg
 359 C/m²). Forestlands contributed the second largest CCSΔSOC (2.429 Tg C) with 151.96% from SH
 360 zone (-26.52–22.86 kg C/m²), and -51.96% from SA zone (-2.96–8.67 kg C/m²). The shrublands only
 361 contributed 7.74% of the total benefit of carbon storage in ΔSOC (1.685 Tg C) with 78.04% from MT-
 362 SA zone (-26.49–30.57 kg C/m²), 45.07% from WT-SA zone (-4.00–3.28 kg C/m²) and -23.11% from
 363 WT-SH zone (-4.60–26.10 kg C/m²).

364 The potential CCSΔSOC by different provinces also changed significantly, but the potential
 365 CCSΔSOC in different ecosystem types by the same provinces were evenly changed (Table S3).
 366 CCSΔSOC increased more in Shanxi and Shaanxi provinces, followed by Henan, Gansu, Inner
 367 Mongolia and Ningxia, and less in Qinghai province.



368 **Figure 76.** Spatial distribution of the CCSΔSOC, (a) the distribution in the whole study area, and
 369 (b) raster level frequency of CCSΔSOC.

370 **Table 2** The ΔSOC (positive and negative portion) in retired farmlands in different ecosystem
 371 types in different climatic zones (Tg C).

<u>Ecosystem types</u>	<u>MT-SA</u>		<u>WT-SA</u>		<u>WT-SH</u>		<u>Total by ecosystems</u>
	<u>Positive</u>	<u>Negative</u>	<u>Positive</u>	<u>Negative</u>	<u>Positive</u>	<u>Negative</u>	
<u>Forestland</u>	<u>1.318</u>	<u>-2.255</u>	<u>0.627</u>	<u>-0.952</u>	<u>6.461</u>	<u>-2.770</u>	<u>2.429</u>
<u>Shrubland</u>	<u>8.502</u>	<u>-6.223</u>	<u>0.369</u>	<u>-1.563</u>	<u>4.868</u>	<u>-4.269</u>	<u>1.685</u>

<u>Grassland</u>	<u>14.543</u>	<u>-0.765</u>	<u>13.196</u>	<u>-5.239</u>	<u>3.545</u>	<u>-7.625</u>	<u>17.657</u>
<u>Total by zones</u>	<u>24.363</u>	<u>-9.243</u>	<u>14.193</u>	<u>-7.753</u>	<u>14.874</u>	<u>-14.664</u>	<u>21.770</u>

372

Table 2 The CCS (positive and negative portion) in retired farmlands in different ecosystem types in different climatic zones (Tg-C).

zone \ type	MT-SA	WT-SA	WT-SH	Total by-ecosystems			
Forestland	1.318	-2.255	0.627	-0.952	6.461	-2.770	2.429
Shrubland	8.502	-6.223	0.369	-1.563	4.868	-4.269	1.685
Grassland	14.543	-0.765	13.196	-5.239	3.545	-7.625	17.657
Total by zones	24.363	-9.243	14.193	-7.753	14.874	-14.664	21.770

373

4. Discussion

374

4.1 Distribution of Retired Farmlands

375

In consideration of the topographic complexity and vegetational variation on the retired farmlands, a large-scale retrieve of retired farmland information from remote sensing images is challenging (Wei et al., 2021). For instance, farmlands and grasslands have similar spectrum characteristics in spring and summer seasons and can be easily confounded (Estel et al., 2015), which lead to inaccuracy in remote sensing image classification. The inaccuracy can be minimized by comparing with multi-source high-resolution remote sensing images (Yan et al., 2023). In this study, although different vegetation types were involved on the retired farmlands (e.g., forestland, shrubland and grassland), the accuracy in identifying retired farmlands could high to 90% by combining visual interpretation of Landsat dataset, field observation, globeland30 database, and ultra-high resolution images from Google Earth.

376

Farmland retirement is the main land use change driver on the Loess Plateau. As classified in this study, retired farmlands on the Loess Plateau from 2000 to 2021 are unevenly distributed across different climatic zones, because of the significant hilly and gully terrain in the study area (Huang et al., 2007; Wen et al., 2015). We focused on forestlands, shrublands and grasslands from retired farmlands, and noticed that most forestlands were distributed in the SH zone due to higher precipitation than the SA zone. Grasslands were more distributed in the MT zone than in the WT zone, due to the temperature in the MT zone being more favorable for grasses than in the WT zone, and people may be more engaged in pastoral activities in the WT zone. Shrublands were more distributed in the MT-SA zone than in the WT-SH zone because the WT-SH zone is more suited to forest growth, thus having high percentage of tree cover and relatively low distribution of shrub. In this study, grasslands accounted for a large proportion in retired farmlands on the Loess Plateau, but the increase in forestlands were more significant.

377

396 The spatial-temporal patterns of farmland retirement varied significantly across years, primarily
397 driven by policy orientation and farmers' participation willingness. Different patterns of retired
398 farmlands among different years were mainly caused by policy orientation and farmers' willingness of
399 participation. During the study period, the Chinese central government implemented two phases
400 of Within the studied period, the central government of China implemented two rounds of GFGP: the
401 first from 1999 to 2013, and the second from 2014 onward in 1999–2013 and 2014–present, respectively.
402 High rates of retirement were observed at the beginning of every phase round due to promising
403 subsidies. High retirement rates were observed at the launch of each phase, largely due to attractive
404 subsidy schemes. However, participation willingness declined afterward, as falling grain prices reduced
405 the relative value of subsidies, leading some farmers to recultivate retired land The farmers' willingness
406 of participation reduced thereafter, and a significant number of farmers chose to reclaim the retired
407 farmlands (Xie et al., 2023). Additionally, population growth between 2000 and 2020 escalated local
408 food demand, further motivating recultivation. Some abandoned farmland-induced misclassification
409 also could introduce bias into the spatial analysis of retired farmlands. These dynamics are consistent
410 with the findings of Wang et al. (2013), who reported a rapid decline in farmland area from 1999 to
411 2003 during the first GFGP phase, followed by a rebound due to recultivation and subsequent
412 stabilization. –

413 4.2 Model development for $CCS\Delta SOC$

414 Land use change due to GFGP can strongly affect SOC, and SOC tend to be lower in farmlands
415 (Deng et al., 2014), which was proved in this study by comparing retired and adjacent unchanged
416 cultivated farmlands. The increase in ΔSOC in retired farmlands shows a strong relationship with the
417 years since retirement, although a slight decrease in SOC may occur during the early stages of land use
418 change The benefits of CCS in the retired farmlands reveals a close relationship to the length of
419 farmland retirement, although a slightly decrease of SOC may be observed in early stage of retirement
420 due to land use change (Deng et al., 2017). During the study period, all vegetation types exhibited a
421 consistent increasing trend in SOC after the initial few years. However, the accumulation tends to
422 approach an upper limit as the ecosystem matures and stabilizes, as observed in grasslands that follow a
423 logarithmic growth pattern. Although in the studied period, all the vegetation types had constant
424 increasing trend after the first few years, the upper limit will be reached when the ecosystem become
425 mature and stable, as showed in grassland with a logarithmic relationship. Some retired farmlands with
426 decreasing SOC were found, which could be explained by interchange of reclamation recultivation and
427 retirement (Qiu et al., 2018), but the deeper mechanism is still need to be explored. Moreover, the high
428 SOC in adjacent farmlands due to good agricultural practice could also offset the benefit of $CCS\Delta SOC$
429 from the GFGP (negative $CCS\Delta SOC$ was mostly found in farmland with high SOC).

430 Based on the statistical analysis (Fig. 4), the range of the $\text{CCS}\Delta\text{SOC}$ in grasslands was
431 significantly smaller than that in forestlands and shrublands. This indicates the accumulation rate of
432 SOC in grasslands was lower than that in forestlands and shrublands due to the low primary productive
433 and the fine quality of grass litter for decomposition (Lukina et al., 2020), whereas woody litter
434 contains more lignin and decomposes slowly (Xiao et al., 2022). Therefore, different models were
435 developed according to vegetation types and climatic zones. Based on the models, the climatic factors
436 had significant effect on $\text{CCS}\Delta\text{SOC}$ besides the length of farmland retirement years since retirement.
437 Among the climatic factors, the models showed that $\text{CCS}\Delta\text{SOC}$ were more sensitive to precipitation-
438 based bioclimatic factors (e.g., *BIO12-BIO19*). This is because most of the Loess Plateau is located in
439 semi-arid and arid area with limited precipitation (Zhang et al., 2015). Moreover, increased
440 precipitation and temperatures can enhance the decomposition of surface litter (Sharma and Sharma,
441 2022), and in turn reduce $\text{CCS}\Delta\text{SOC}$.

442 4.3 Benefits in $\text{CCS}\Delta\text{SOC}$ on the Loess Plateau

443 Under climate change, ecological restoration is an urgent need to improve the healthiness of
444 degraded ecosystems (Liu et al., 2023; Yang et al., 2023). As a major benefit from ecological
445 restoration, the increase in SOC ($\text{CCS}\Delta\text{SOC}$) brings a lot of interests due to SOC is the major carbon
446 pool in the ecosystems. To illustrate $\text{CCS}\Delta\text{SOC}$ from ecological restoration, only a comparison of
447 restored and adjacent unrestored ecosystems should be persuasive (Francaviglia et al., 2019). Numbers
448 of studies focusing on $\text{CCS}\Delta\text{SOC}$ in retired farmlands has been conducted on the Loess Plateau, and
449 found an increasing $\text{CCS}\Delta\text{SOC}$ as a result of GFGP (Wang et al., 2021b), and the national SOC
450 sequestration caused by retirement was estimated to be 14.46 Tg per year (Zhao et al., 2013). But they
451 failed to make comparison with the adjacent farmlands. In this study, we analyzed the $\text{CCS}\Delta\text{SOC}$ of
452 retired farmlands and adjacent in-use cultivated farmlands, and confirmed that the GFGP can provide
453 significant amount of $\text{CCS}\Delta\text{SOC}$ on the Loess Plateau, although negative $\text{CCS}\Delta\text{SOC}$ was found in
454 some areas.

455 Recently, studies have shown that SOC stocks in the GFGP region on the Loess Plateau increased
456 by 20.18 Tg C between 1982 and 2017 (Li et al., 2022). The total $\text{CCS}\Delta\text{SOC}$ (21.77 Tg C) of retired
457 farmlands on the Loess Plateau estimated in this study was slightly higher than that value, which
458 proved that the results of this study are reliable. Although the mechanisms driving of $\text{CCS}\Delta\text{SOC}$ vary
459 across vegetation restoration types and climatic zones. While warmer and more humid regions
460 generally exhibit higher carbon sequestration rates—owing to enhanced photosynthesis and plant
461 growth under favorable temperature and precipitation regimes—these conditions also accelerate SOC
462 turnover, potentially limiting long-term storage benefits compared to arid and semi-arid regions (Sierra
463 et al., 2017). Therefore, selecting appropriate vegetation types is critical to prevent slow SOC

464 accumulation and early saturation. Moreover, sustainable management practices—such as controlled
465 grazing and systematic harvesting—are essential to maintain ecosystem health and maximize long-term
466 soil carbon storage, thereby strengthening the role of retired farmlands in climate change mitigation~~are~~
467 ~~different for different vegetation restoration types in different climatic zones, the rate of carbon~~
468 ~~sequestration was higher in warm and humid areas than in cold or arid areas because of high~~
469 ~~temperatures and sufficient precipitation induced strong photosynthesis and rapid plant growth.~~
470 However, long time carbon storage in soil is essential in mitigate climate change. The high turnover
471 rate of SOC in warm and humid areas may limit the benefit in carbon storage than in arid and semi arid
472 regions (Sierra et al., 2017).

473 4.4 Limitations and Uncertainties

474 Remote sensing images are widely used in studies of land use change because of their accuracy
475 and timeliness. In this study, the use of Landsat dataset has practical feasibility to provide reliable
476 distribution of retired farmlands. However, the Loess Plateau has a large spatial area, and has a
477 fragmented and complex topography, which increases the difficulty of land use classification.
478 Therefore, the 30_m resolution images can result in misclassification (e.g., abandoned farmlands vs
479 retired farmlands), although we obtained acceptable accuracy (80%–91%). Recently, the availability of
480 ultra-high resolution images (sub-meter resolution) allows a more accurate classification, but lacks of
481 long period records.

482 In this study, the direct comparison of retired farmlands and adjacent cultivated farmlands
483 reflected a more persuasive CCSΔSOC. The multivariate linear regression models that developed for
484 estimating CCSΔSOC can effectively reduce estimation errors by accounting for the spatial
485 heterogeneity of the Loess Plateau~~reduce the estimation error in the consideration of the spatial~~
486 ~~heterogeneity on the Loess Plateau. Increasing the number of sample points would further enhance~~
487 model flexibility, allowing the incorporation of additional factors—such as slope, elevation, and soil
488 properties—to stratify the study area into more representative subzones. Furthermore, establishing
489 permanent observation points to monitor both retired and adjacent cultivated farmlands would provide
490 reliable pairwise comparisons essential for robust model calibration. However~~To more accurately~~
491 project the future soil carbon sequestration potential of retired farmlands, the integration,~~to predict the~~
492 ~~future potential of soil carbon sequestration in the retired farmlands on the Loess Plateau, the assistant~~
493 of process-based ecosystem models could be more reliable~~a more reliable approach~~, such as DLEM
494 (Dynamic Land Ecosystem Model, (Tian et al., 2003)), LPJ-GUESS (Lund Potsdam Jena General
495 Ecosystem Simulator, (Smith et al., 2001)), and CENTURY (Parton et al., 1987).

496 5. Conclusions

497 Farmland retirement is an effective strategy to restore degraded ecosystems and increase carbon

498 storage on the Loess Plateau. In this study, we found the total area of retired farmlands on the Loess
499 Plateau during the study period was 39,065 km². The dominant ecosystem type was grasslands,
500 followed by shrublands and forestlands. The area of retired farmlands showed significant interannual
501 changes without a specific trend, and the retired farmlands varied in different ~~climate zone~~climatic
502 zones. Area of retired farmlands in the MT-SA zone were significantly higher than WT-SA zone and
503 WT-SH zone. Based on soil samples, we found that CCSΔSOC increased with the ~~length of farmland~~
504 ~~retirement~~years since retirement, and developed seven regression models for CCSΔSOC by ~~length of~~
505 ~~farmland~~retirementyears since retirement, temperature, precipitation, soil bulk density, latitude and
506 longitude, and ecosystem types. According to the models, the total benefits in CCSΔSOC from retired
507 farmlands on the Loess Plateau were estimated to be 21.77 Tg C, with the variation ranged from -26.52
508 to 31.91 kg C/m² at grid cell level. The most CCSΔSOC were contributed by retired farmlands in the
509 MT-SA zone (15.120 Tg C), followed by WT-SA zone (6.440 Tg C) and WT-SH zone (0.210 Tg C).
510 Therefore, Long-term implementation of GFGP brought significant impacts on increasing soil carbon
511 sinks on the Loess Plateau, which contributed significantly in mitigating climate changes and
512 promoting sustainability in the studied area.

513 **Competing interests**

514 The authors declare no competing interests.

515 **Data availability**

516 The associated datasets are available at Figshare (<https://doi.org/10.6084/m9.figshare.28785971>,
517 ~~Yang, 2025~~), including distribution of retired farmlands from 2000 to 2021, ~~length of farmland~~
518 ~~retirement~~years since retirement, and high resolution CCSΔSOC from the retired farmlands.

519 **Author contribution**

520 BG: data curation, investigation, methodology, formal analysis, validation and visualization; MF:
521 investigation, formal analysis and validation; LY: data curation; TG, CM, XH, ZG, ZM: resources and
522 visualization; QL: funding acquisition and conceptualization; ZW: resources; WL: Conceptualization,
523 methodology, project administration and supervision. BG and WL: Writing – original draft preparation;
524 All authors: Writing – review & editing.

525 **Acknowledgements**

526 This study was funded by the National Key Research and Development Program of China
527 (2022YFF1302200). The authors would like to thank all the reviewers who participated in the review.

528 **Reference**

529 Bai, R., Wang, X., Li, J., Yang, F., Shangguan, Z., and Deng, L. Area Datasets of ‘Grain for Green’
530 Project in Counties of the Loess Plateau from 1999 to 2020[DS/OL]. V1. Science Data Bank.,
531 <https://cstr.cn/31253.11.sciencedb.j00001.00820>. CSTR:31253.11.sciencedb.j00001.00820. 2024.
532 Calmon, M., Brancalion, P. H., Paese, A., Aronson, J., Castro, P., da Silva, S. C., and Rodrigues, R. R.:

533 Emerging threats and opportunities for large-scale ecological restoration in the Atlantic Forest of
534 Brazil, *Restor. Ecol.*, 19, 154-158, <https://doi.org/10.1111/j.1526-100X.2011.00772.x>, 2011.

535 Cui, W., Liu, J., Jia, J., and Wang, P.: Terrestrial ecological restoration in China: identifying advances
536 and gaps, *Environ. Sci. Eur.*, 33, 1-14, <https://doi.org/10.1186/s12302-021-00563-2>, 2021.

537 de Oliveira Faria, C. and Magrini, A.: Biodiversity Governance from a Cross-Level and Cross-Scale
538 Perspective: The case of the Atlantic Forest biome in Brazil, *Environm. Policy Govern.*, 26, 468-
539 481, <https://doi.org/10.1002/eet.1728>, 2016.

540 Deng, L., Liu, G. b., and Shangguan, Z. p.: Land-use conversion and changing soil carbon stocks in C
541 hina's 'Grain-for-Green' Program: a synthesis, *Global Change Biol.*, 20, 3544-3556,
542 <https://doi.org/10.1111/gcb.12508>, 2014.

543 Deng, L., Liu, S., Kim, D. G., Peng, C., Sweeney, S., and Shangguan, Z.: Past and future carbon
544 sequestration benefits of China's grain for green program, *Global Environm. Change*, 47, 13-20,
545 <https://doi.org/10.1016/j.gloenvcha.2017.09.006>, 2017.

546 Estel, S., Kuemmerle, T., Alcántara, C., Levers, C., Prishchepov, A., and Hostert, P.: Mapping farmland
547 abandonment and recultivation across Europe using MODIS NDVI time series, *Remote Sens.*
548 *Environ.*, 163, 312-325, <https://doi.org/10.1016/j.rse.2015.03.028>, 2015.

549 Feng, X., Fu, B., Lu, N., Zeng, Y., and Wu, B.: How ecological restoration alters ecosystem services: an
550 analysis of carbon sequestration in China's Loess Plateau, *Sci. Rep.*, 3, 2846,
551 <https://doi.org/10.1038/srep02846>, 2013.

552 Ferreira, C. S., Seifollahi-Aghmiuni, S., Destouni, G., Ghajarnia, N., and Kalantari, Z.: Soil
553 degradation in the European Mediterranean region: Processes, status and consequences, *Sci. Total*
554 *Environ.*, 805, 150106, <https://doi.org/10.1016/j.scitotenv.2021.150106>, 2022.

555 Francaviglia, R., Álvaro-Fuentes, J., Di Bene, C., Gai, L., Regina, K., and Turtola, E.: Diversified
556 arable cropping systems and management schemes in selected European regions have positive
557 effects on soil organic carbon content, *Agriculture*, 9, 261,
558 <https://doi.org/10.3390/agriculture9120261>, 2019.

559 Graham, F.: Daily briefing: How to shore up Africa's Great Green Wall, *Nature*,
560 <https://doi.org/10.1038/d41586-022-01247-4>, 2022.

561 Huang, M., Gong, J., Shi, Z., Liu, C., and Zhang, L.: Genetic algorithm-based decision tree classifier
562 for remote sensing mapping with SPOT-5 data in the HongShiMao watershed of the loess plateau,
563 China, *Neural. Comput. Appl.*, 16, 513-517, <https://doi.org/10.1007/s00521-007-0104-z>, 2007.

564 Lengefeld, E., Metternicht, G., and Nedungadi, P.: Behavior change and sustainability of ecological
565 restoration projects, *Restor. Ecol.*, 28, 724-729, <https://doi.org/10.1111/rec.13159>, 2020.

566 [Li, B., Li, P., Yang, X., Xiao, H., Xu, M., Liu, G. Land-use conversion changes deep soil organic](https://doi.org/10.1002/ldr.3644)
567 [carbon stock in the Chinese Loess Plateau\[J\]. *Land Degradation & Development*, 32\(1\): 505-517,](https://doi.org/10.1002/ldr.3644)
568 [https://doi.org/10.1002/ldr.3644, 2020.](https://doi.org/10.1002/ldr.3644)

569 Li, H., Wu, Y., Liu, S., Zhao, W., Xiao, J., Winowiecki, L. A., Vågen, T.-G., Xu, J., Yin, X., and Wang,
570 F.: The Grain-for-Green project offsets warming-induced soil organic carbon loss and increases soil
571 carbon stock in Chinese Loess Plateau, *Sci. Total Environ.*, 837, 155469,
572 <https://doi.org/10.1016/j.scitotenv.2022.155469>, 2022.

573 Liu, C., Jia, X., Ren, L., Zhao, C., Yao, Y., Zhang, Y., and Shao, M. a.: Cropland-to-shrubland
574 conversion reduces soil water storage and contributes little to soil carbon sequestration in a dryland
575 area, *Agric., Ecosyst. Environ.*, 354, 108572, <https://doi.org/10.1016/j.agee.2023.108572>, 2023.

576 Lu, F., Hu, H., Sun, W., Zhu, J., Liu, G., Zhou, W., Zhang, Q., Shi, P., Liu, X., and Wu, X.: Effects of

577 national ecological restoration projects on carbon sequestration in China from 2001 to 2010, Proc.
578 Nat. Acad. Sci., 115, 4039-4044, <https://doi.org/10.1073/pnas.1700294115>, 2018.

579 Lukina, N., Kuznetsova, A., Tikhonova, E., Smirnov, V., Danilova, M., Gornov, A., Bakhmet, O.,
580 Kryshen, A., Tebenkova, D., and Shashkov, M.: Linking forest vegetation and soil carbon stock in
581 Northwestern Russia, *Forests*, 11, 979, <https://doi.org/10.3390/f11090979>, 2020.

582 ~~Ma, R., Wang, D., Cui, X., Yao, X., Li, S., Wang, H., and Liu, B.: Distribution and driving force of~~
583 ~~water use efficiency under vegetation restoration on the Loess Plateau, *Remote Sens.*, 14, 4513,~~
584 ~~<https://doi.org/10.3390/rs14184513>, 2022.~~

585 Macia, E., Allouche, J., Sagna, M. B., Diallo, A. H., Boëtsch, G., Guisse, A., Sarr, P., Cesaro, J.-D., and
586 Duboz, P.: The Great Green Wall in Senegal: questioning the idea of acceleration through the
587 conflicting temporalities of politics and nature among the Sahelian populations, *Ecol. Society*, 28,
588 31, <https://doi.org/10.5751/ES-13937-280131>, 2023.

589 Mir, Y. H., Ganie, M. A., Shah, T. I., Aezum, A. M., Bangroo, S. A., Mir, S. A., Dar, S. R., Mahdi, S. S.,
590 Baba, Z. A., and Shah, A. M.: Soil organic carbon pools and carbon management index under
591 different land use systems in North western Himalayas, *PeerJ*, 11, e15266,
592 <https://doi.org/10.7717/peerj.15266>, 2023.

593 Ouyang, Z., Zheng, H., Xiao, Y., Polasky, S., Liu, J., Xu, W., Wang, Q., Zhang, L., Xiao, Y., and Rao,
594 E.: Improvements in ecosystem services from investments in natural capital, *Science*, 352, 1455-
595 1459, <https://doi.org/10.1126/science.aaf2295>, 2016.

596 Pape, T.: Futuristic restoration as a policy tool for environmental justice objectives, *Restor. Ecol.*, 30,
597 e13629, <https://doi.org/10.1111/rec.13629>, 2022.

598 Parton, W. J., Schimel, D. S., Cole, C. V., and Ojima, D. S.: Analysis of factors controlling soil organic
599 matter levels in Great Plains grasslands, *Soil Sci. Soc. Am. J.*, 51, 1173-1179,
600 <https://doi.org/10.2136/sssaj1987.03615995005100050015x>, 1987.

601 Paustian, K., Collier, S., Baldock, J., Burgess, R., Creque, J., DeLonge, M., Dungait, J., Ellert, B.,
602 Frank, S., and Goddard, T.: Quantifying carbon for agricultural soil management: from the current
603 status toward a global soil information system, *Carbon Manage.*, 10, 567-587,
604 <https://doi.org/10.1080/17583004.2019.1633231>, 2019.

605 Piffer, P. R., Calaboni, A., Rosa, M. R., Schwartz, N. B., Tambosi, L. R., and Uriarte, M.: Ephemeral
606 forest regeneration limits carbon sequestration potential in the Brazilian Atlantic Forest, *Global
607 Change Biol.*, 28, 630-643, <https://doi.org/10.1111/gcb.15944>, 2022.

608 Prăvălie, R., Patriche, C., Borrelli, P., Panagos, P., Roșca, B., Dumitrașcu, M., Nita, I.-A., Săvulescu, I.,
609 Birsan, M.-V., and Bandoc, G.: Arable lands under the pressure of multiple land degradation
610 processes. A global perspective, *Environ. Res.*, 194, 110697,
611 <https://doi.org/10.1016/j.envres.2020.110697>, 2021.

612 Qiu, B., Zou, F., Chen, C., Tang, Z., Zhong, J., and Yan, X.: Automatic mapping afforestation, cropland
613 reclamation and variations in cropping intensity in central east China during 2001–2016, *Ecol.
614 Indic.*, 91, 490-502, <https://doi.org/10.1016/j.ecolind.2018.04.010>, 2018.

615 Scharlemann, J. P., Tanner, E. V., Hiederer, R., and Kapos, V.: Global soil carbon: understanding and
616 managing the largest terrestrial carbon pool, *Carbon Manage.*, 5, 81-91,
617 <https://doi.org/10.4155/cmt.13.77>, 2014.

618 Shao, M., Adnan, M., Zhang, L., Liu, P., Cao, J., and Qin, X.: Carbonate mineral dissolution and its
619 carbon sink effect in Chinese loess, *Land*, 12, 133, <https://doi.org/10.3390/land12010133>, 2022.

620 Sharma, G. and Sharma, L.: Climate change effect on soil carbon stock in different land use types in

621 eastern Rajasthan, India, *Environm. Dev. Sustain.*, 24, 4942-4962, [https://doi.org/10.1007/s10668-](https://doi.org/10.1007/s10668-021-01641-4)
622 [021-01641-4](https://doi.org/10.1007/s10668-021-01641-4), 2022.

623 Sierra, C. A., Malghani, S., and Loescher, H. W.: Interactions among temperature, moisture, and
624 oxygen concentrations in controlling decomposition rates in a boreal forest soil, *Biogeosciences*,
625 14, 703-710, <https://doi.org/10.5194/bg-14-703-2017>, 2017.

626 Smith, B., Prentice, I. C., and Sykes, M. T.: Representation of vegetation dynamics in the modelling of
627 terrestrial ecosystems: comparing two contrasting approaches within European climate space, *Glob.*
628 *Ecol. Biogeogr.*, 621-637, <https://doi.org/https://www.jstor.org/stable/3182691>, 2001.

629 Sun, Y., Zhu, J., Yan, Q., Hu, Z., and Zheng, X.: Changes in vegetation carbon stocks between 1978
630 and 2007 in central Loess Plateau, China, *Environ. Earth Sci.*, 75, 1-16,
631 <https://doi.org/10.1007/s12665-015-5199-4>, 2016.

632 Tian, H., Melillo, J. M., Kicklighter, D. W., Pan, S., Liu, J., McGuire, A. D., and Moore III, B.:
633 Regional carbon dynamics in monsoon Asia and its implications for the global carbon cycle, *Glob.*
634 *Planet. Change*, 37, 201-217, [https://doi.org/10.1016/S0921-8181\(02\)00205-9](https://doi.org/10.1016/S0921-8181(02)00205-9), 2003.

635 Wang, L., Li, Z., Wang, D., Chen, J., Liu, Y., Nie, X., Zhang, Y., Ning, K., and Hu, X.: Unbalanced
636 social-ecological development within the Dongting Lake basin: Inspiration from evaluation of
637 ecological restoration projects, *J. Cleaner Prod.*, 315, 128161,
638 <https://doi.org/10.1016/j.agee.2021.107636>, 2021b.

639 Wang, J., Liu, Z., Gao, J., Emanuele, L., Ren, Y., Shao, M., and Wei, X.: The Grain for Green project
640 eliminated the effect of soil erosion on organic carbon on China's Loess Plateau between 1980 and
641 2008, *Agric., Ecosyst. Environ.*, 322, 107636, <https://doi.org/10.1016/j.jclepro.2021.128161>, 2021a.

642 Wang, B., Liu, G., Zhang, G., and Yang, Y. Effects of Grain for Green Project on Food Security on
643 Loess Plateau. *Bulletin of Soil and Water Conservation*, 33(3), 241-245,
644 <https://doi.org/10.13961/j.cnki.stbctb.2013.03.059>, 2013. (In Chinese with English abstract)

645 ~~Wang, L., Li, Z., Wang, D., Chen, J., Liu, Y., Nie, X., Zhang, Y., Ning, K., and Hu, X.: Unbalanced~~
646 ~~social-ecological development within the Dongting Lake basin: Inspiration from evaluation of~~
647 ~~ecological restoration projects, *J. Cleaner Prod.*, 315, 128161,~~
648 ~~<https://doi.org/10.1016/j.agee.2021.107636>, 2021b.~~

649 Wei, Z., Gu, X., Sun, Q., Hu, X., and Gao, Y.: Analysis of the spatial and temporal pattern of changes
650 in abandoned farmland based on long time series of remote sensing data, *Remote Sens.*, 13, 2549,
651 <https://doi.org/10.3390/rs13132549>, 2021.

652 Wen, W., Wang, Y., Yang, L., Liang, D., Chen, L., Liu, J., and Zhu, A.-X.: Mapping soil organic carbon
653 using auxiliary environmental covariates in a typical watershed in the Loess Plateau of China: a
654 comparative study based on three kriging methods and a soil land inference model (SoLIM),
655 *Environ. Earth Sci.*, 73, 239-251, <https://doi.org/10.1007/s12665-014-3518-9>, 2015.

656 Xiao, J.: Satellite evidence for significant biophysical consequences of the "Grain for Green" Program
657 on the Loess Plateau in China, *J. Geophys. Res.:Biogeosci.*, 119, 2261-2275,
658 <https://doi.org/10.1002/2014JG002820>, 2014.

659 Xiao, Y., Huang, Z., Ling, Y., Cai, S., Zeng, B., Liang, S., and Wang, X.: Effects of forest vegetation
660 restoration on soil organic carbon and its labile fractions in the Danxia landform of China,
661 *Sustainability*, 14, 12283, <https://doi.org/10.3390/su141912283>, 2022.

662 Xie, Y., Ma, Z., Fang, M., Liu, W., Yu, F., Tian, J., Zhang, S., and Yan, Y.: Analysis of Net Primary
663 Productivity of Retired Farmlands in the Grain-for-Green Project in China from 2011 to 2020,
664 *Land*, 12, 1078, <https://doi.org/10.3390/land12051078>, 2023.

665 Xu, C., Jiang, Y., Su, Z., Liu, Y., and Lyu, J.: Assessing the impacts of Grain-for-Green Programme on
666 ecosystem services in Jinghe River basin, China, *Ecol. Indic.*, 137, 108757,
667 <https://doi.org/10.1016/j.ecolind.2022.108757>, 2022.

668 Xu, X., Liu, J., Zhang, S., Li, R., Yan, C., and Wu, S. China Multi-Temporal Land Use Remote Sensing
669 Monitoring Dataset (CNLUCC). Resource and Environment Science Data Platform.
670 <https://www.resdc.cn/DOI/DOI.aspx?DOIID=54>. <https://doi.org/10.12078/2018070201>, 2018.

671 Yan, X., Li, J., Smith, A. R., Yang, D., Ma, T., and Su, Y.: Rapid land cover classification using a 36-
672 year time series of multi-source remote sensing data, *Land*, 12, 2149,
673 <https://doi.org/10.1016/j.ecolind.2022.108757>, 2023.

674 Yang, J., Huang, X. The 30 m annual land cover dataset and its dynamics in China from 1990 to 2019.
675 *Earth System Science Data*. 13(8), 3907-3925, <https://doi.org/10.5194/essd-13-3907-2021>, 2021.

676 Yang, Y., Sun, H., Zhang, P., Wu, F., Qiao, J., Li, T., Wang, Y., and An, S.: Review of managing soil
677 organic C sequestration from vegetation restoration on the Loess Plateau, *Forests*, 14, 1964,
678 <https://doi.org/10.3390/f14101964>, 2023.

679 ~~Yang, . leilei .: The 30 meter resolution distribution of retired farmlands and their carbon sequestration~~
680 ~~on the Loess Plateau in China from 2000 to 2021, Figshare[data set].~~
681 ~~<https://doi.org/10.6084/m9.figshare.28785971>, 2025.~~ Yi, P., Wu, H., Hu, B., Wen, X., Han, H.,
682 Cheng, X.. Variation characteristics and influencing factors of soil organic carbon storage after
683 returning farmland to forest on the Loess Plateau. *Acta Ecologica Sinica*, 2023, 43(24): 10054-
684 10064, <https://doi.org/10.20103/j.stxb.202306241340>, 2023. (in Chinese with English abstract).

685 Zhang, F., Li, C., Wang, Z., Glidden, S., Grogan, D. S., Li, X., Cheng, Y., and Frohling, S.: Modeling
686 impacts of management on farmland soil carbon dynamics along a climate gradient in Northwest
687 China during 1981–2000, *Ecol. Modell.*, 312, 1-10,
688 <https://doi.org/10.1016/j.ecolmodel.2015.05.006>, 2015.

689 Zhang, K., Yihe, L., Bojie, F., and Ting, L.: The effects of restoration on vegetation trends:
690 spatiotemporal variability and influencing factors, *Earth Environ. Sci. Trans. R. Soc. Edinburgh*,
691 109, 473–481, <https://doi.org/10.1017/S1755691018000518>, 2018.

692 Zhang, Q., Lu, J., Xu, X., Ren, X., Wang, J., Chai, X., and Wang, W.: Spatial and temporal patterns of
693 carbon and water use efficiency on the loess plateau and their influencing factors, *Land*, 12, 77,
694 <https://doi.org/10.3390/land12010077>, 2022.

695 Zhao, F., Chen, S., Han, X., Yang, G., Feng, Y., and Ren, G.: Policy-guided nationwide ecological
696 recovery: Soil carbon sequestration changes associated with the Grain-to-Green Program in China,
697 *Soil Sci.*, 178, 550-555, <https://doi.org/10.1097/SS.000000000000018>, 2013.

698 Zhou, R., Pan, X., Wei, H., Xie, X., Wang, C., Liu, Y., Li, Y., and Shi, R.: Soil organic carbon stocks in
699 terrestrial ecosystems of China: revised estimation on three-dimensional surfaces, *Sustainability*, 8,
700 1003, <https://doi.org/10.3390/su8101003>, 2016.

701